

# **Absence of diffuse double layer effect on the vibrational properties and oxidation of chemisorbed carbon monoxide on a Pt(111) electrode**

*Marta C. Figueiredo<sup>a</sup>, Dennis Hiltrop<sup>b</sup>, Ravishankar Sundararaman<sup>c</sup>, Kathleen A. Schwarz<sup>d</sup>,  
Marc T.M. Koper<sup>a,\*</sup>*

<sup>a</sup> Leiden Institute of Chemistry, Leiden University, P.O. Box 9502, 2300 RA Leiden, The Netherlands

<sup>b</sup> Laboratory of Industrial Chemistry, Ruhr-Universität Bochum, Universitätsstr. 150, 44780 Bochum, Germany

<sup>c</sup> Department of Materials Science and Engineering, Rensselaer Polytechnic Institute, Troy, NY 12189, USA

<sup>d</sup> Material Measurement Laboratory, National Institute of Standards and Technology, Gaithersburg, MD 20899, USA

## **\*Corresponding author:**

Marc T. M. Koper

m.koper@lic.leidenuniv.nl

## **Abstract:**

In this work we investigate the effects of the diffuse double layer thickness on the electrochemical Stark tuning and oxidation of carbon monoxide at Pt(111) surfaces in perchloric acid solution. The diffuse double layer thickness was modified by changing the concentration (ionic strength) of the supporting electrolyte. The Stark tuning slope of the adsorbed CO was evaluated with Fourier Transformed Infrared Spectroscopy, and the CO oxidation was monitored with cyclic voltammetry. The results show that both electrochemical Stark tuning and oxidation are independent of the HClO<sub>4</sub> concentration of the supporting electrolyte, revealing the absence of diffuse layer effects on the aqueous Pt(111)/CO system. By comparison to previously reported theoretical calculations, we attribute this insensitivity to the special double layer structure of Pt(111)/CO, in which the potential drop occurs primarily between the terminating oxygen of the adsorbed CO adlayer

and first water layer of the electrolyte, making the properties of adsorbed CO nearly independent of the ionic strength of the electrolyte.

## **Introduction**

The electrical double layer (EDL) refers to the spatial distribution of ionic charges near the interface of a charged surface in contact with a liquid electrolyte<sup>1-2</sup>. Conventionally, the EDL is divided into two separate spatial regions, Helmholtz layer, and an outer diffuse or Gouy-Chapman layer. The Helmholtz layer is the plane of closest approach of ions to the electrode surface. In the presence of specific adsorption the Helmholtz layer is divided into two parts, the Inner Helmholtz Plane (IHP), defined by specifically adsorbed ions, and the Outer Helmholtz Plane (OHP), defined by the plane of closest approach on non-specifically adsorbed ions. Non-specifically adsorbed ions at the OHP are fully solvated, and interact electrostatically with the charged surface.

The diffuse layer is the outermost part of the EDL region in which fully solvated ions are distributed in a Debye-Hückel-type fashion interacting electrostatically with the charged surface. The electrode surface charge is effectively screened by the counter charge in the EDL, and hence the potential drop between (metal) electrode and the electrolyte effectively occurs within this EDL<sup>2</sup>. Understanding the structure of the electrochemical double layer (EDL) and its influence on electrochemical reactions has been one of the core challenges in physical electrochemistry.

In classical electrochemical kinetics, the EDL effect is expressed by the so-called Frumkin correction<sup>3-8</sup>. The idea of the Frumkin double-layer correction is that the effective potential difference driving charge transfer is the potential difference between the metal and the reaction plane somewhere inside the EDL, and not the entire potential drop across the EDL. The potential in the reaction plane, the so-called  $\phi_2$  potential, should be sensitive to the concentration of the electrolyte, as this affects the capacitance of the diffuse Gouy-Chapman part of the EDL and thereby changes the potential distribution between inner and diffuse parts of the EDL. Although there are many papers on the Frumkin correction for “outer-

sphere-type” electron transfer reactions<sup>8-13</sup>, there are only a few studies considering these “diffuse double layer effects” in electrocatalysis<sup>14-15</sup>.

One of the most frequently studied model reactions in electrocatalysis is the adsorption and electro-oxidation of carbon monoxide (CO) on a Pt electrode. Mechanistic aspects of CO adsorption and oxidation on Pt have been well described in the literature<sup>16</sup>. This system can be followed by spectroscopic methods allowing the in-situ observation of the Pt/CO interactions when changing the structure of the double layer. As an adsorbed species, the C-O vibrational stretching frequency depends on the potential applied to the electrode, an effect known as the electrochemical Stark effect<sup>17</sup>. The change in the C-O stretching frequency with potential, the Stark tuning rate, is primarily determined by the electronic transfer between orbitals of the electrode and the CO adsorbate (enhanced back donation between the electronic d states of the metal to the  $2\pi^*$  adsorbate state when the potential is made more negative) and changes of the molecular polarizability under the electric field, i.e. the interaction of the interfacial electric field with the dipole moment of the adsorbate.<sup>17-20</sup> We will refer to the change in vibrational features of adsorbates on electrodes as a consequence of a change in the electrode potential as the “electrochemical Stark effect”, to distinguish it from the pure Stark effect. The electrochemical Stark effect includes both effects referred to above: changes induced by changes in the chemical bonding, and changes due to changes in the interfacial electric field.<sup>21</sup> The Pt/CO system has previously been used to study double layer effects in organic electrolytes<sup>22</sup>. The advantage of organic solvents is that they allow a wide range of potentials to access the electrochemical Stark tuning rate, due to the inhibition of water reduction and CO oxidation. Roth and Weaver found that the CO Stark tuning rate in organic solvents with an electrolyte of alkali salt is essentially independent of the supporting electrolyte cation and supporting electrolyte concentration. Similar studies have not yet been performed for the aqueous environment, despite water-based electrolytes being the most commonly used in electrochemistry and electrocatalysis. More importantly, the effect of double layer structure on CO monolayer oxidation, which does not occur in the absence of water, has not yet been reported.

Therefore, in this work, we study the influence of the double layer structure, in aqueous media, on the electrochemical Stark tuning rate and on the oxidation of CO chemisorbed on Pt(111) electrodes, by employing in situ Fourier Transformed Infrared (FTIR) Spectroscopy

and cyclic voltammetry (CV). We use different supporting electrolyte concentrations to vary the thickness of the diffuse layer and thereby the local potential distribution and corresponding electric field. Interestingly, we find that both CO bond characteristics (as observed through its C-O vibrational Stark tuning rate) and CO monolayer oxidation exhibit no diffuse double layer effect, similar to the data reported for organic solvents<sup>22</sup>. Supported by measurements of the interfacial capacitance and our recent Density Functional Theory calculations of the Pt(111)-CO/electrolyte interface,<sup>23</sup> we argue that the absence of diffuse double layer effects is due to the fact that the CO monolayer changes the EDL structure compared to the “clean” Pt(111) surface by generating a hydrophobic low-capacitance interfacial layer that dominates the potential drop inside the EDL.

### **Experimental:**

The voltammetric experiments were performed at room temperature in a three-electrode configuration using a Pt (111) bead of 2 mm diameter (from icryst<sup>a</sup>) as working electrode, a Pt wire as counter and a reversible hydrogen electrode (RHE) as reference electrode. The electrolyte solutions were prepared using different concentrations of HClO<sub>4</sub> (70%, Merck Suprapur<sup>®</sup>) and ultrapure water (Merck Millipore<sup>®</sup>, 18.2 MΩ cm). The electrochemical measurements were performed with the working electrode in hanging meniscus configuration and the potential was controlled with an Autolab PGSTAT302N potentiostat. The current density reported represents the measured current normalized to the electrochemical surface area of the working electrode. To ensure the proper surface ordering, the electrodes were prepared as previously described<sup>24-25</sup>. Briefly, prior to each measurement, the crystals were flame-annealed and cooled to room temperature in an Ar:H<sub>2</sub> (3:1) environment. Subsequently, the crystal was protected with a drop of water saturated in the same gas mixture and

---

<sup>a</sup> Certain commercial materials are identified in this paper to foster understanding. Such identification does not imply recommendation or endorsement by the National Institute of Standards and Technology, nor does it imply that the materials or equipment identified are necessarily the best available for the purpose

transferred to the electrochemical cell. All the experiments were performed by first acquiring a blank voltammogram of the Pt(111) in the electrolyte solution purged with Ar (6.0 Linde), to ensure the surface cleanliness and order. After recording the blank, CO (6.0 Linde) was purged in the solution for 2 minutes to ensure a full layer of CO on the electrode surface, and subsequently Ar was purged for 20 minutes through the electrolyte solution in order to remove all the CO from solution. During this process the electrode potential was kept at 0.1 V (vs RHE) to avoid CO oxidation. After all CO was removed from the solution, FTIR measurements were performed and cyclic voltammograms for CO stripping were recorded. For the *in-situ* spectroscopy FTIR measurements, a Bruker Vertex 80v vacuum spectrometer was used, with an MCT detector and *p*-polarized light, in the external reflection configuration. A CaF<sub>2</sub> prism bevelled at 60 ° was used. The spectra were obtained in a thin layer configuration in which the electrode was pressed against the prismatic window, at 0.1 V (vs RHE). Next, the electrode potential was changed and the sample spectrum was obtained. Each spectrum represents the average of 100 interferograms collected with a resolution of 4 cm<sup>-1</sup>. The spectra are shown as (R-R<sub>0</sub>)/R<sub>0</sub>, where R and R<sub>0</sub> are the reflectance at the sample and reference potential, respectively. The working electrode for these measurements was a disk of 6 mm diameter from Mateck. The procedures used for the electrode treatment, blank voltammetry and CO stripping experiments were the same as for the electrochemical measurements.

## Results

### *FTIR spectroscopy - CO adsorption*

In order to evaluate the effect of the diffuse layer thickness on the electrochemical Stark tuning rate of adsorbed CO, we collected FTIR spectra of CO adsorbed on Pt(111), in HClO<sub>4</sub> electrolyte, at electrolyte concentrations of: 1 mM, 10 mM, 100 mM, and 500 mM (note: M has been used to represent the SI unit mol/L) . In Figure 1, the spectra obtained for adsorbed CO on Pt(111) with 0.1 M HClO<sub>4</sub> at different electrode potentials are presented. The reference spectrum was taken at 0.9 V vs RHE, as at this potential all the CO has been oxidized from the surface. The results show the presence of two bands at 2074-2052 cm<sup>-1</sup> and 1853-1830 cm<sup>-1</sup>, corresponding to atop and bridge adsorbed CO, respectively, in accordance with previous publications<sup>22, 26-27</sup>. These bands are observed in the potential range between

0.1 V to 0.6 V vs RHE. At higher potentials ( $>0.6$  V), CO oxidation takes place and the vibrational bands are no longer observed.

As expected, the vibrational frequency shifts to higher wavenumbers with increasing potential. The positive electrochemical Stark tuning rate has been attributed predominantly to the decrease of the electronic back donation between Pt d states and the  $2\pi^*$  orbital of the chemisorbed CO with more positive potential<sup>19-20</sup>. This effect will lead to the shortening of the C-O bond shifting its internal stretching frequency to higher wavenumbers.

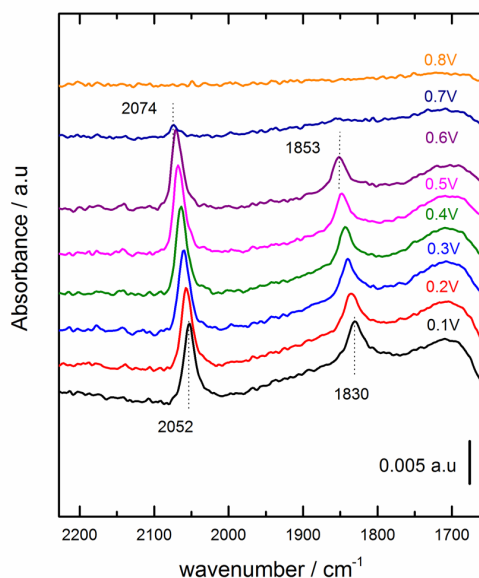


**Figure 1: FTIR spectra of CO adsorbed on Pt(111) in 0.1 M HClO<sub>4</sub> at different electrode potentials. Background spectrum taken at 0.9 V vs RHE. Data offset along the y axes for clarity.**

The electrochemical Stark tuning rate was determined for different concentrations of supporting electrolyte to evaluate the effect of the diffuse layer thickness on the vibrational properties of the adsorbed CO. The vibrational frequencies for CO (bridge and atop) at different electrode potentials are plotted in Figure 2 for five different concentrations of HClO<sub>4</sub>. The results are presented on the standard hydrogen potential (SHE) scale because the vibrational properties of the CO are expected to be independent of the proton chemical potential.

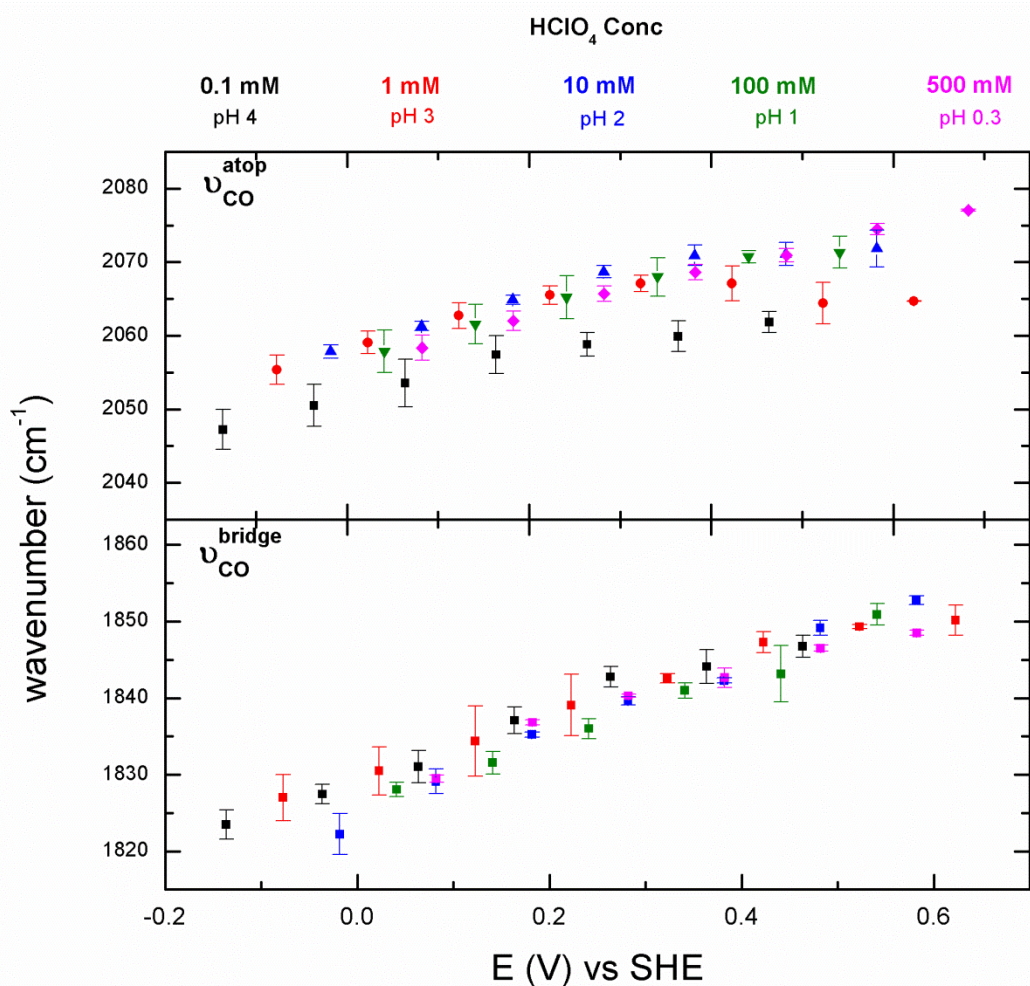


**Figure 2: Vibrational frequencies obtained from the FTIR results at different electrode potentials (vs SHE) for 500, 100, 10, 1 and 0.1 mM HClO<sub>4</sub>. The error bars correspond to the standard deviation of at least three different measurements.**

Figure 2 shows a linear dependence of the vibrational frequency of adsorbed CO on the potential, which appears to be independent of the concentration of inert electrolyte. In fact, the vibration frequencies in the different electrolyte concentrations are almost identical, within the experimental error, suggesting a very small dependence of the CO adsorption properties on the ionic strength of the electrolyte. From the vibrational frequencies presented in Figure 2, electrochemical Stark tuning rates were obtained and are presented in Figure 3.

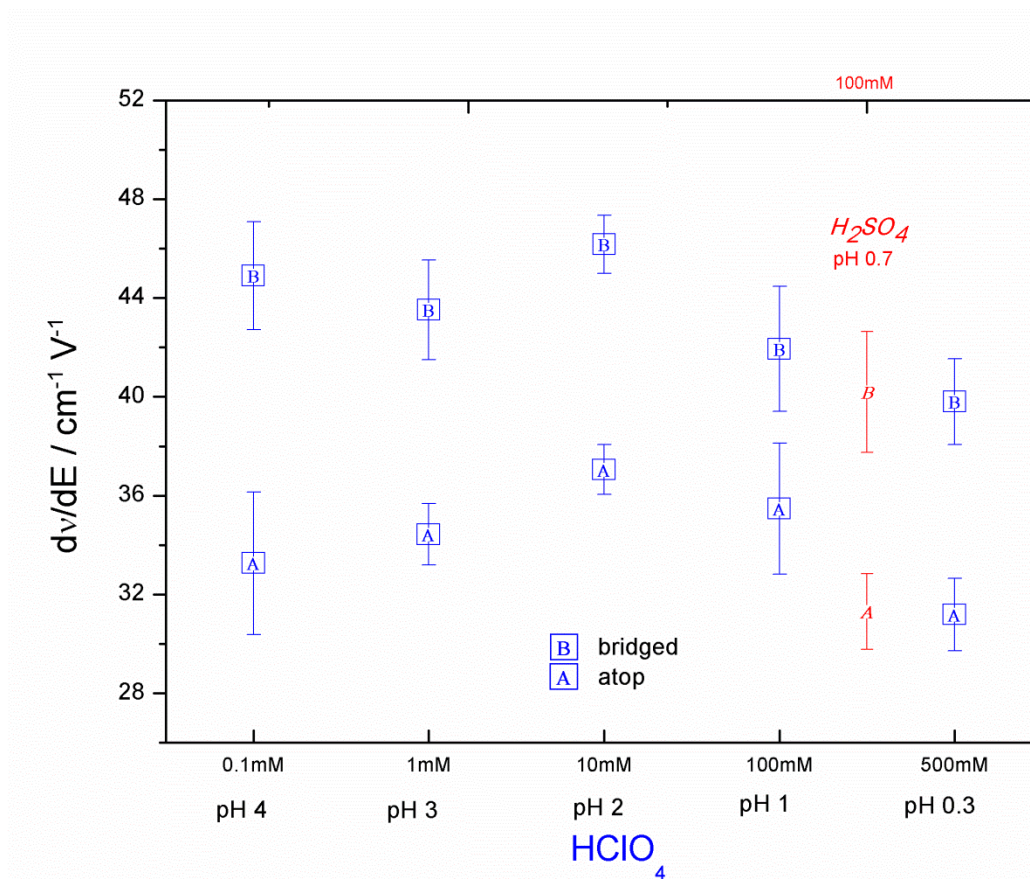


**Figure 3: Electrochemical Stark tuning rates for CO adsorbed bridge and atop for different HClO<sub>4</sub> concentrations. The error bars correspond to the propagated error for the slope in the linear fit of the data in Figure 2.**

The observed electrochemical Stark tuning rates of 40-46 cm<sup>-1</sup> V<sup>-1</sup> for bridged CO and 32-36 cm<sup>-1</sup> V<sup>-1</sup> for atop CO are in good agreement with previous reports for both the experimental and theoretical Stark tuning rates of CO on Pt(111) single crystals<sup>19-22,28</sup>. However, the Stark tuning rates presented in Figure 3 are essentially independent of electrolyte concentration (within the experimental error). Small differences in the values are probably due to differences in pH and deviation from exact linearity over the entire potential range shown in Figure 2. For comparison between two different supporting electrolytes, Stark tuning rates were also measured for 100 mM H<sub>2</sub>SO<sub>4</sub> (red points in the graph). The Stark tuning shift for CO with H<sub>2</sub>SO<sub>4</sub> (pH 0.7) is between that of CO with HClO<sub>4</sub> at pH 0.3 and 1. As both electrolytes have a very similar ionic strength the results suggest that the small differences in the Stark tuning rate observed in Figure 3 are not due to differences in diffuse layer thickness. Publications dealing with the systematic effect of electrolyte pH on the vibration

properties of CO on metal electrodes are scarce<sup>15,29</sup>. Theoretical studies predict that for CO on Pt(111) the Stark rate could increase by as much as ca.  $30 \text{ cm}^{-1} \text{ V}^{-1}$  from pH=2 to pH=12, and that this increase is due to a negative shift on the absolute potential scale.<sup>30</sup> This apparent pH dependence is then essentially the result of a possible nonlinearity of the electrochemical Stark tuning rate when measured over a wide potential window. Such nonlinearity cannot be concluded on the basis of the data presented in Fig.2.

A similar independence of the electrochemical Stark tuning rate on the electrolyte concentration was observed by Weaver et al.<sup>22</sup> in non-aqueous electrolytes such as acetonitrile, methanol and THF. In that study, the role of the double layer cations on the vibrational properties of CO on Pt was evaluated in organic solvents. Organic solvents are suitable for such studies owing to their wider accessible potential window. The Stark tuning rate was found to be nearly independent of the solvent used and electrolyte concentration, but a small dependence was found on the size of tetraalkylammonium cations, with a decrease of the  $\nu_{\text{CO}} - E$  slopes for bigger cations. No dependence of the electrochemical Stark tuning rate on different alkali metal cations was found.

#### *Electrochemistry - CO oxidation*

To obtain further information on the effect of the diffuse double layer on Pt(111) in the presence and absence of adsorbed CO, capacitance measurements were performed (Table 1). As previously reported<sup>23</sup>, the capacitance values for the Pt(111)/CO interface are much lower than that of the bare pure Pt (111) surface and nearly independent of the electrolyte concentration. The blank voltammograms for Pt(111) in different HClO<sub>4</sub> concentrations are presented in Figure 4A. The blank CVs illustrate the absence of an effect of both ionic strength and pH on the hydrogen adsorption region ( $0.06 \text{ V} < E < 0.4 \text{ V}$ ) (small differences are due to an Ohmic drop effect when the electrolyte concentration is low). However, the size of the sharp peaks in the OH region near 0.8 V vs. RHE decreases with decreasing acid concentration (in contrast to Fig.2, we use the RHE scale in Fig.4 as the chemical reactions taking place at the electrode are pH dependent). We have recently argued on the basis of in situ Shell-Isolated Nanoparticle Enhanced Raman Spectroscopy (SHINERS) measurements that there is a (weak) interaction between perchlorate and the chemisorbed OH layer on

Pt(111), and this may result in a change of the shape of the OH peak with different perchlorate concentration <sup>31</sup>.

**Table 1: Capacitance values extracted from measurements of the current density at 0.4 V at different scan rates for Pt(111) and Pt(111)/CO <sup>23</sup>**

HClO <sub>4</sub> conc. (mmol/L)	Capacitance (μF/cm <sup>2</sup> )	
	Pt(111)	Pt(111)/CO
1	70.2±1.5	11.0±0.3
10	85.2±1.1	10.8±0.5
100	106.0±1.9	11.2±0.7

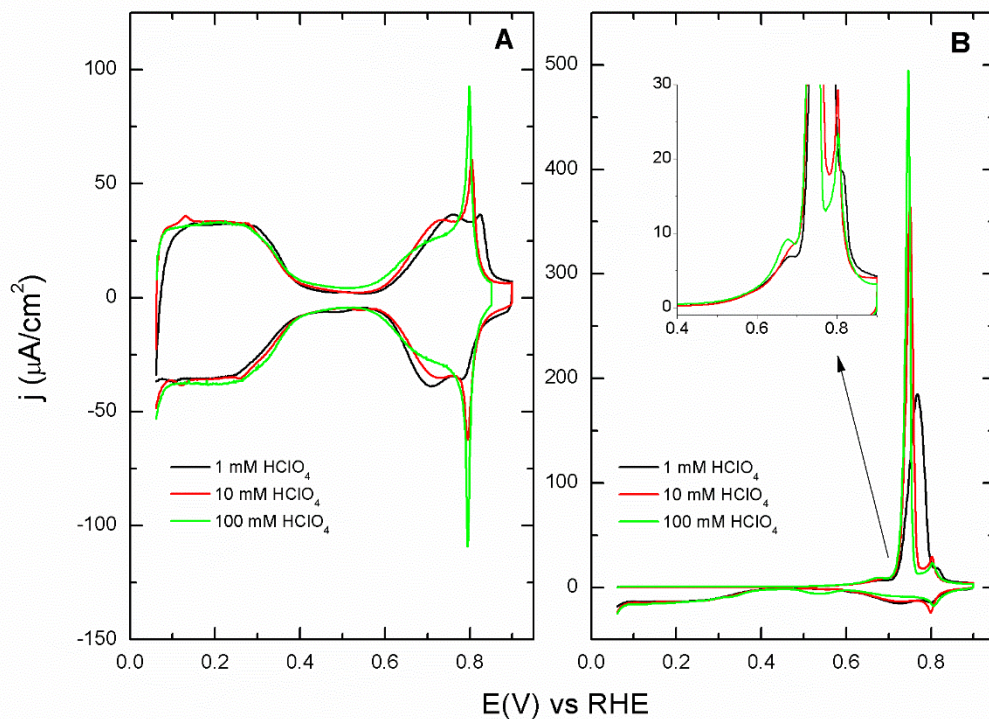


**Figure 4: CVs for Pt(111) A) for different concentrations of HClO<sub>4</sub> (0.05 Vs<sup>-1</sup>) and B) for the oxidation of adsorbed CO at different HClO<sub>4</sub> concentrations (0.02Vs<sup>-1</sup>). CO reacts with hydroxide, so the onset potentials are constant on the RHE scale, which holds the potential fixed relative to the proton chemical potential.**

CVs for Pt(111)/CO<sub>ads</sub> measured with different supporting electrolyte concentrations are presented in Figure 4B. The results show that, regardless of the acid concentration, the surface is fully blocked by CO from 0.06 V to 0.5 V (vs. RHE) as revealed by the absence of current for H adsorption and the characteristic profile for Pt(111) in HClO<sub>4</sub> solutions. From 0.5 V, oxidation of the CO layer starts taking place. In fact, the onset potential for the oxidation is exactly the same for the three HClO<sub>4</sub> concentrations (see inset in Figure 4B), revealing that the onset of the electrochemical reaction is also independent of the concentration of ions nearby the surface and the diffuse double layer thickness. The oxidation peak itself shows differences both in shape and maximum current density for 100 mM, 10 mM and 1 mM. These differences are not surprising as the Ohmic resistance of the electrolyte for the low concentration solutions is very significant (~11 MΩ) and will therefore strongly affect the actual potential of the electrode. Yet, the major observation from Figure 4B is the independence of the (initial) rate of the CO oxidation reaction on the diffuse double layer.

## Discussion

The results described above show that both the vibrational properties of chemisorbed CO (as measured by the Stark tuning slope) and CO oxidation are independent of the supporting electrolyte concentration used in the experiments and consequently independent of the solution's ionic strength. These observations suggest that the properties of CO at the surface are independent of the diffuse layer thickness, and that there is no need for a Frumkin correction for the CO oxidation rate. In other words, the  $\phi_2$  potential relevant for CO oxidation does not change with the diffuse double layer properties. Similarly, the capacitance of the Pt(111)/CO<sub>ads</sub> interface is nearly independent of the electrolyte concentration, in contrast to the capacitance of the “clean” Pt(111) surface which shows a clear Gouy-Chapman contribution<sup>23</sup>. However, we recently suggested an explanation for this concentration independence of the Pt(111)/CO<sub>ads</sub> capacitance compared to that of the “clean”

Pt(111) surface<sup>23</sup> based on first-principles calculations of the spatial distribution of the electrostatic potential.

For “clean” Pt(111) most of the Helmholtz layer potential drop occurs between the outermost surface atom and the liquid electrolyte; this capacitance is large enough that the decrease in the Gouy-Chapman “outer” layer capacitance still has a sizeable effect on the overall capacitance of the interface<sup>23</sup> However, for the Pt(111)/CO interface, the net Helmholtz layer capacitance is much smaller, reducing the relative capacitance contribution of the Gouy-Chapman outer layer to the total capacitance. As explained in our previous publication<sup>23</sup>, the total capacitance of the interface can be computed from a series connection of capacitors for different regions, and the lower capacitance will dominate the overall capacitance. The capacitance values reported on Table 1 were obtained in the double layer region of Pt(111) (0.4V vs RHE), which is relatively far from the pzc of a Pt(111)-CO electrode (ca. 1.1 V vs SHE)<sup>34</sup>. Under these conditions, the value of the Gouy-Chapman capacitance will be larger than its value close to the pzc, making it a smaller relative contribution to the total capacitance. Therefore, changes in the diffuse capacitance will be less apparent in measurements of the total capacitance (see e.g. Fig. 3 in ref.23).

Remarkably, the potential drop across the CO adlayer is rather modest, indicating that the CO should be seen as an extension of the metal surface rather than as a dielectric spacer with a very low dielectric constant.<sup>22, 32</sup> The low capacitance of Pt(111)/CO interface is instead due to the potential drop between the terminating O of the adsorbed CO and the electrolyte, which have a larger separation than in the Pt-electrolyte case because of the hydrophobic interaction between the CO adlayer and the liquid. This leads to an overall capacitance (at 0.1 M) of the Pt(111)/CO interface that is much smaller than that of the Pt(111) interface (11  $\mu\text{F}/\text{cm}^2$  vs 30  $\mu\text{F}/\text{cm}^2$ , respectively)<sup>33, 34</sup>. These calculations suggest that the total capacitance of the Pt(111)/CO interface is low not because the CO acts as an insulating spacer, but because the CO-modified surface repels the solvent.

The dominance of the potential drop between the CO and the electrolyte may explain why the electrochemical Stark tuning rates measured in the FTIR experiments, and the onset potentials of CO oxidation measured in the CV experiments, are independent of the

electrolyte concentration and show no diffuse layer effects. We also note that the potential of zero charge of the CO-covered Pt(111) is outside of our voltage window (leading to a higher Gouy-Chapman capacitance), and this may also contribute to the apparent absence of a double layer effect.<sup>23</sup>

## Conclusions

In this work, we investigated the properties of carbon monoxide (CO) and its oxidation, on a Pt(111) electrode at multiple electrolyte concentrations in order to evaluate the effect of the diffuse layer thickness on the properties of adsorbed CO. Our results revealed that the electrochemical Stark tuning rates are independent of the ionic strength of the supporting electrolyte and the diffuse layer thickness. A similar insensitivity was found for CO oxidation, the onset potential of which is independent of the electrolyte ionic strength. We explain these results by the low double layer capacity of the Pt(111)-CO interface. We showed recently that the low capacitance of the Pt-CO interface is primarily the result of the existence of a very low “gap” capacitance that occurs between the oxygen of the adsorbed CO and the solvent, which is due to a strongly hydrophobic interaction between the CO and the liquid. The dominance of this “gap” capacitance causes the insensitivity of the CO adlayer to changes in the outer Gouy-Chapman layer and, as a consequence, no diffuse double layer effects are observed for CO adsorption and oxidation on Pt(111).

## Acknowledgements

D.H. acknowledges the support of the Cluster of Excellence RESOLV (EXC 1069) funded by the Deutsche Forschungsgemeinschaft.

## References:

1. Timmer, B.; Sluyters-Rehbach, M.; Sluyters, J. H., Electrode kinetics and double layer structure. *Surface Science* **1969**, *18* (1), 44-61.
2. Parsons, R., The electrical double layer: recent experimental and theoretical developments. *Chemical Reviews* **1990**, *90* (5), 813-826.
3. Frumkin, A., Wasserstoffüberspannung und Struktur der Doppelschicht. In *Zeitschrift für Physikalische Chemie*, 1933; Vol. 164A, p 121.

4. Nazmutdinov, R. R.; Tsirlina, G. A.; Petrii, O. A.; Kharkats, Y. I.; Kuznetsov, A. M., Quantum chemical modelling of the heterogeneous electron transfer: from qualitative analysis to a polarization curve. *Electrochimica Acta* **2000**, *45* (21), 3521-3536.
5. Tsirlina, G. A.; Petrii, O. A.; Nazmutdinov, R. R.; Glukhov, D. V., Frumkin Correction: Microscopic View. *Russ J Electrochem* **2002**, *38* (2), 132-140.
6. Rusanova, M. Y.; Tsirlina, G. A.; Nazmutdinov, R. R.; Fawcett, W. R., Role of Charge Distribution in the Reactant and Product in Double Layer Effects: Construction of Corrected Tafel Plots. *The Journal of Physical Chemistry A* **2005**, *109* (7), 1348-1356.
7. Breiter, M.; Kleinerman, M.; Delahay, P., Structure of the Double Layer and Electrode Processes1. *Journal of the American Chemical Society* **1958**, *80* (19), 5111-5117.
8. Gavaghan, D. J.; Feldberg, S. W., Extended electron transfer and the Frumkin correction. *Journal of Electroanalytical Chemistry* **2000**, *491* (1), 103-110.
9. Ahmed, S. M., Studies of the double layer at oxide-solution interface. *The Journal of Physical Chemistry* **1969**, *73* (11), 3546-3555.
10. Dickinson, E. J. F.; Compton, R. G., Influence of the diffuse double layer on steady-state voltammetry. *Journal of Electroanalytical Chemistry* **2011**, *661* (1), 198-212.
11. Royea, W. J.; Krüger, O.; Lewis, N. S., Frumkin corrections for heterogeneous rate constants at semiconducting electrodes. *Journal of Electroanalytical Chemistry* **1997**, *438* (1-2), 191-197.
12. Yamakata, A.; Osawa, M., Cation-dependent restructure of the electric double layer on CO-covered Pt electrodes: Difference between hydrophilic and hydrophobic cations. *Journal of Electroanalytical Chemistry* **2016**.
13. Velasco-Velez, J.-J.; Wu, C. H.; Pascal, T. A.; Wan, L. F.; Guo, J.; Prendergast, D.; Salmeron, M., The structure of interfacial water on gold electrodes studied by x-ray absorption spectroscopy. *Science* **2014**, *346* (6211), 831-834.
14. Ataka, K.-i.; Yotsuyanagi, T.; Osawa, M., Potential-Dependent Reorientation of Water Molecules at an Electrode/Electrolyte Interface Studied by Surface-Enhanced Infrared Absorption Spectroscopy. *The Journal of Physical Chemistry* **1996**, *100* (25), 10664-10672.
15. Lopes, P. P.; Strmcnik, D.; Jirkovsky, J. S.; Connell, J. G.; Stamenkovic, V.; Markovic, N., Double layer effects in electrocatalysis: The oxygen reduction reaction and ethanol oxidation reaction on Au(111), Pt(111) and Ir(111) in alkaline media containing Na and Li cations. *Catalysis Today* **2016**, *262*, 41-47.
16. Koper, M. T. M.; Lai, S. C. S.; Herrero, E., Mechanisms of the Oxidation of Carbon Monoxide and Small Organic Molecules at Metal Electrodes. In Koper M.T.M., Ed., *Fuel Cell Catalysis*, John Wiley & Sons, Inc.: 2008; pp 159-207.
17. Holloway, S.; Nørskov, J. K., Changes in the vibrational frequencies of adsorbed molecules due to an applied electric field. *Journal of Electroanalytical Chemistry and Interfacial Electrochemistry* **1984**, *161* (1), 193-198.
18. Lambert, D. K., Vibrational Stark effect of CO on Ni(100), and CO in the aqueous double layer: Experiment, theory, and models. *The Journal of Chemical Physics* **1988**, *89* (6), 3847-3860.
19. Koper, M. T. M.; Santen, R. A. v.; Wasileski, S. A.; Weaver, M. J., Field-dependent chemisorption of carbon monoxide and nitric oxide on platinum-group (111) surfaces: Quantum chemical calculations compared with infrared spectroscopy at

- electrochemical and vacuum-based interfaces. *The Journal of Chemical Physics* **2000**, *113* (10), 4392-4407.
20. Koper, M. T. M.; van Santen, R. A., Electric field effects on CO and NO adsorption at the Pt(111) surface. *Journal of Electroanalytical Chemistry* **1999**, *476* (1), 64-70.
21. Wasileski, S.; Koper, M. T. M.; Weaver, M. J.; Field-Dependent Electrode–Chemisorbate Bonding: Sensitivity of Vibrational Stark Effect and Binding Energetics to Nature of Surface Coordination, *Journal of American Chemical Society* **2002**, *124* (1) 2796-2805
22. Roth, J. D.; Weaver, M. J., Role of double-layer cation on the potential-dependent stretching frequencies and binding geometries of carbon monoxide at platinum–nonaqueous interfaces. *Langmuir* **1992**, *8* (5), 1451-1458.
23. Sundararaman, R.; Figueiredo, M. C.; Koper, M. T. M.; Schwarz, K., Electrochemical capacitance of CO-terminated Pt(111) is dominated by CO-solvent gap. *The Journal of Physical Chemistry Letters* **2017**, *8*, 5344-5348
24. Clavilier, J.; Actii, K. E.; Petit, M.; Rodes, A.; Zamakhchari, M. A., Electrochemical monitoring of the thermal reordering of platinum single-crystal surfaces after metallographic polishing from the early stage to the equilibrium surfaces. *Journal of Electroanalytical Chemistry and Interfacial Electrochemistry* **1990**, *295* (1–2), 333-356.
25. Arán-Ais, R. M.; Figueiredo, M. C.; Vidal-Iglesias, F. J.; Climent, V.; Herrero, E.; Feliu, J. M., On the behavior of the Pt(100) and vicinal surfaces in alkaline media. *Electrochimica Acta* **2011**, *58* (0), 184-192.
26. Heyden, B. E.; Bradshaw, A. M., The adsorption of CO on Pt(111) studied by infrared reflection—Absorption spectroscopy. *Surface Science* **1983**, *125* (3), 787-802.
27. Kinomoto, Y.; Watanabe, S.; Takahashi, M.; Ito, M., Infrared spectra of CO adsorbed on Pt(100), Pt(111), and Pt(110) electrode surfaces. *Surface Science* **1991**, *242* (1–3), 538-543.
28. Marković, N. M.; Lucas, C. A.; Rodes, A.; Stamenković, V.; Ross, P. N., Surface electrochemistry of CO on Pt(1 1 1): anion effects. *Surface Science* **2002**, *499* (2–3), L149-L158.
29. Weaver, M. J.; Zou, S.; Tang, C., A concerted assessment of potential-dependent vibrational frequencies for nitric oxide and carbon monoxide adlayers on low-index platinum-group surfaces in electrochemical compared with ultrahigh vacuum environments: Structural and electrostatic implications. *The Journal of Chemical Physics* **1999**, *111* (1), 368-381.
30. Uddin, J.; Anderson, A. B., Trends with coverage and pH in Stark tuning rates for CO on Pt(1 1 1) electrodes. *Electrochimica Acta* **2013**, *108*, 398-403.
31. Huang, Y.-F.; Kooyman, P. J.; Koper, M. T. M., Intermediate stages of electrochemical oxidation of single-crystalline platinum revealed by in situ Raman spectroscopy. *Nature Communications*, **2016**, *7*, 12440.
32. Rice, C.; Wieckowski, A.; Oldfield, E.; A Detailed NMR-Based Model for CO on Pt Catalysts in an Electrochemical Environment: Shifts, Relaxation, Back-Bonding, and the Fermi-Level Local Density of States, *Journal of American Chemical Society*, **2000**, *122*, 1123-1129

33. Weaver, M.; Potentials of Zero Charge for Platinum(111)–Aqueous Interfaces: A Combined Assessment from In-Situ and Ultrahigh-Vacuum Measurements, *Langmuir*, **1998**, 14, 3932-3936
34. Cuesta, A.; Measurement of the surface charge density of CO-saturated Pt(111) electrodes as a function of potential: the potential of zero charge of Pt(111), *Surface Science*, **2014**, 572, 11-22